Published in final edited form as:
Epilepsy Behav. 2009 January ; 14(Suppl 1): 39–46. doi:10.1016/j.yebeh.2008.09.008.

Detecting seizure origin using basic, multiscale population dynamic measures: Preliminary findings

A.K. Roopun[a], **R.D. Traub**[b], **T. Baldeweg**[c], **M.O. Cunningham**[a], **R.G. Whittaker**[a], **A. Trevelyan**[a], **R. Duncan**[d], **A.J.C. Russell**[d], and **M.A. Whittington**[a,*]

[a] Institute of Neuroscience, The Medical School, Newcastle University, Framlington Place, Newcastle upon Tyne NE2 4HH, UK

[b] IBM T.J. Watson Research Center, Yorktown Heights, NY 10589, USA

[c] Institute of Child Health, University College London, London WC1N 1EH, UK

[d] Department of Clinical Neurophysiology, Institute of Neurological Sciences, Southern General Hospital, Glasgow G51 4TF, UK

Abstract

Many types of electrographic seizures are readily identifiable by direct visual examination of electroencephalographic or electrocorticographic recordings. This process can, however, be painstakingly slow, and much effort has been expended to automate the process using various dynamic properties of epileptiform waveforms. As methods have become more subtle and powerful they have been used for seizure subclassification, seizure prediction, and seizure onset identification and localization. Here we concentrate on the last, with reference to seizures of neocortical origin. We briefly review some of the methods used and introduce preliminary results from a very simple dynamic model based on key electrophysiological properties found in some seizure types: occurrence of very fast oscillations (sometimes called *ripples*), excess gamma frequency oscillations, electroencephalographic/electrocorticographic flattening, and changes in global synchrony. We show how this multiscale analysis may reveal features unique to seizure onset and speculate on the underlying cellular and network phenomena responsible.

Keywords

Focal epilepsy; Neocortex; Seizure onset detection; Seizure localization

1. Introduction

Detecting electrographic changes associated with seizures in patients with drug-intractable epilepsy is a critical component of the “workup” to surgery. Painstaking, epoch-by-epoch analysis of a patient's electroencephalogram (EEG), followed by more detailed analysis of periseizure recordings may guide surgical intervention toward specific problem areas in the absence of clear imaging and semiological clues. Conventional dipole models of surface EEGs, however, may give “ghost” sources, and rarely localize seizures with sufficient spatial resolution to accurately guide surgical resection. More detailed analysis of the dynamics of

*Corresponding author. m.a.whittington@ncl.ac.uk (M.A. Whittington)..

5. Conflict of interest statement
The authors here declare that the development of this study does not imply any kind of conflict of interest.

seizure events has been used, or at least proposed as useful, for more than 40 years [1]. Simple linear analysis has been used extensively and shown to capture some of the features of seizure foci quite robustly. For example cross-correlations may determine the location of some epileptogenic foci [2], and changes in the relative scale of higher compared with lower EEG frequencies can be a reliable indicator of cortical neuronal state [3] and have been shown to signal the start of seizures in many cases [4]. Also, rule-based methods have proved very robust in separating epileptiform events from background [5]. Wavelet-based analyses, examining frequency changes on multiple scales, have taken this approach further, successfully detecting seizures with reduced false positives [6]. Principal component analyses, and other methods dependent on correlation matrices, have also been used to compare across multiple concurrent channels of data and have been shown to be useful in detection of abnormal EEG signatures of epilepsy [7,8]. More complex and mathematically elegant methods often use nonlinear time series analysis to more accurately reflect the nature of electrographic data. Nonlinear patterns of synchrony may often reveal very different degrees of intercortical temporal interaction associated with seizures when compared with linear methods [9].

Any method for localizing epileptic foci must include a feature for detecting the precise time at which transition from normal to ictaform activity occurs. Once this is achieved, it is then possible to identify the location (electrode number) of the initial transition and plot its spread to neighboring cortical areas (electrodes). This is a nontrivial problem, particularly evidenced by the power of nonlinear analytical techniques to quantify very subtle changes in cortical dynamics. The main issue is one of time scale: Simple linear methods such as power spectral density show abrupt (on the order of 0.1 second) changes in dynamics [10] at onset of electrographic seizures. However, many dynamic analyses can detect changes several tens of seconds before the electrographic event [11]. In addition, variations on nonlinear, spatiotemporal correlations have shown clear changes in cortical dynamics some tens of *minutes* before seizures [12-14]. These long-term changes may flag alterations in the plastic state of neuronal networks or—not mutually exclusively—perhaps slow changes in homeostatic state of discrete cortical regions. Riding on top of these changes are presumed to be alterations in more rapid response states in networks that predispose highly localized cortical regions to fulminant changes in dynamic state (see below). It is the signature of these short time scale events that this article considers in more detail.

Within the above framework we must ask which dynamic features of electrographic data can signal these short time scale changes. The onset of electrographic seizures often manifests as high-amplitude EEG signals with abrupt appearance of prominent high-frequency events (80 Hz to several hundreds of hertz, very fast oscillations (VFOs), or ripples) that are rarely seen in normal intracranial EEG records, suggesting a specific relationship to electrographic seizures [15]. In focal epilepsies, VFOs are prevalent immediately prior to seizure generation and are spatially constrained to the cortical seizure focus [4,16-21]. In addition, gamma frequency oscillations (30–80 Hz) have been reported to occur suddenly at high amplitude in many temporal lobe epilepsies [22-24]. As with VFOs, gamma rhythms appear to signal local changes, in terms of both their power [23] and their pattern of phase synchronization [25]. Although there is some semantic confusion over the nature of VFOs and gamma rhythms—VFO sometimes being referred to also as a type of gamma rhythm [26]—it is clear from in vitro studies that these two EEG bands have different underlying cellular and network mechanisms [27], with gamma rhythms critically dependent on synaptic inhibition and VFOs (variously “high gamma,” ripples, high-frequency oscillations) being generated by gap junctional connections in networks of neurons [28]. They will therefore be treated separately in the present study.

In addition to the sudden increase in higher-frequency EEG bands (gamma and VFO, above), many focal electrographic seizures are accompanied by a decrease in low-frequency EEG

bands, termed the *electrodecremental response* [4]. However, the interrelationship between low- and high-frequency bands is variable between patients with temporal lobe epilepsy. An initial slow wave at the start of the electrographic seizure may or may not be present with the faster rhythms, and different apparent origins of these initial slow waves, when present, are associated with different modal frequencies of accompanying faster rhythms [29,30]. In each case a different underlying mechanism of seizure generation is proposed.

Finally, for a focal seizure to manifest clinically, activity must spread from the point (or points) of origin to generate an experiential, motor, or behavioral correlate. We therefore wished to combine measures of the aforementioned four features (VFO, gamma, decreased slow rhythms, and synchrony) of some focal electrographic seizures to see whether these factors alone were sufficient to signal a rapid change in cortical dynamics unique to seizure onset. From this we attempted to see whether such a combined measure could be of possible use in focus localization.

2. Methods

Subdural recordings were made from a 32- or 48-contact platinum array (Ad-Tech) placed over the region of neocortex identified as the putative focus from scalp EEG measures and seizure semiology in two patients. Recordings were made using either Neuroscan or Xltek equipment, with output bandwidth up to 1 kHz (patient A) or 500 Hz (patient B) with a reference on a distant contact on the subdural strip; the EEG was then re-referenced to a common average signal. Patient A was a 5-year-old girl with history of seizures from a few weeks postpartum. Magnetic resonance imaging (MRI) revealed a lesion in the right frontal lobe. A detailed patient history is provided elsewhere [31]. Patient B was an 11-year-old boy with seizures from soon after birth. MRI showed an abnormal gyral pattern in the left inferior frontal gyrus. All recordings were carried out with approval of the local ethics committees responsible.

Electrocorticographic data were analyzed with the accent on computational simplicity: simpler routines are less time consuming. Although the presented data are very preliminary, the goal of this approach is ultimately to have a near real-time readout of focus location perioperatively. Briefly, each channel of data was filtered into three bands. FIR filters were used with low order (<200) to optimize the speed of the process, though this resulted in some overlap between bands. VFO was defined as 80–500 Hz, gamma as 30–80 Hz, and low-frequency rhythms as 1–30 Hz. Bandpass-filtered data were then windowed at length 500 ms and offset by 50 ms throughout the recording. Multitaper spectral density estimates were obtained for each window, and the peak power spectral density within each band was plotted over time (see Fig. 2b–d). Finally, the broadband signal (1–500 Hz) was used to construct an estimate of global synchrony using simple linear measures. Synchrony was quantified as the mean height of the cross-correlation, at 0 ms, between each electrode and all other electrodes, again using the windowing and offset parameters above. Thus, positive values indicate the degree of zero-phase synchrony, and negative values, the degree of antiphase synchrony. It has been shown previously that bandpass synchronization measures perform better than broadband measures [25]. With this simple (and quick) method there is some degree of interdependence between the absolute power of each signal and the synchronization measure. Using broadband allowed us to minimize this cross-talk and also avoided any prior assumptions about the specific spectral components responsible for any synchrony changes seen. For example, this technique would be expected to be biased in favor of large-amplitude, lower-frequency events rather than the high-frequency components. However, such components are very much reduced in electrodecremental responses (see Results), and early attempts at seizure onset detection using only high-frequency, bandpass-filtered data failed to distinguish between seizure onset and late afterdischarges (data not shown).

An index of when activity patterns changed on each channel was constructed with the a priori assumption (from the evidence cited in the Introduction) that electrographic seizure onset was associated with a change in the ratio of higher to lower EEG frequencies concurrently with an increase in global synchrony. As mentioned above, we considered gamma and VFO bands to constitute different (though not entirely independent) processes. Although both increases and decreases in synchrony have been quantified [10], we wished to concentrate on increase synchronization as a measure of communication from presumed focus to neighboring cortical areas. Thus, our focus index measure (FI), at any given time window on each channel, is the ratio of the product of the VFO and gamma powers and the low-frequency band power, multiplied by the global synchrony measure for that channel.

3. Results

Raw electrocorticographic recordings show bursts of VFO and gamma rhythms on many channels, often simultaneously. Long (several seconds) runs of these high-frequency rhythms occur around the subjective estimate of electrographic seizure onset (Fig. 1). However, any quantitative measure or seizure onset must distinguish between the high-frequency activity associated with interictal-like bursts and physiological sharp waves, the occurrence of which may or may not be related to the underlying epilepsy, and that associated with seizure onset (see expanded recording, Fig. 1). Use of measurements taken on multiple frequency scales was proposed to be of possible use in this respect (see Fig. 2). Furthermore, in setting out to quantify seizure onset alone, we needed to find a measure any change in which was unique to this time point.

As shown in many previous studies, simple measures of cortical dynamics do not readily provide a feature unique to focal seizure onset, though it should be noted that analysis routines can be “trained” to ignore interictal-like events [4]. This can clearly be seen in Fig. 2, which summarizes the measures used for channel 21 in patient A. VFO power alone (Fig. 2B) shows local maxima associated with the initial interictal-like event 12 seconds into the recording, a more prolonged rise at 17 seconds, and peaks corresponding to each late afterdischarge following the full electrographic seizure event. So, although this measure shows highly significant deviations from background levels (the few seconds of preictal, baseline activity immediately preceding seizure, $P < 0.01$) it does not, alone, distinguish between interictal events and the beginning and later stages of ictal events in this example. The situation is even less clear-cut when considering the gamma band (Fig. 2C). Again there are local maxima approximately coexistent with those of the VFO power, but background, preictal gamma rhythms are very much evident, and these maxima only just reach significance when compared with mean baseline levels ($P < 0.05$). In the more classic EEG frequency range (1–30 Hz), mean power initially decreased during the electrographic seizure (baseline 2.4 ± 0.4 vs $1.1 \pm 0.2 \times 10^6\ \mu^2$, $P < 0.05$) before increasing dramatically during the overt repetitive bursting seen during the seizure proper. Global synchrony was low preictally, with a mean value for this channel of -0.8 ± 0.3, perhaps reflecting the decrease in synchronization seen before seizures previously [32]. Although no abrupt change in this measure was seen during the subjective time of seizure onset, there was a gradual shift to high positive values from circa 10–20 seconds into the recording that decreased back toward baseline as the seizure progressed.

The preceding examples illustrate the absence of a clear dynamic signature for electrographic seizure onset with each measure taken alone. However, the aim was to combine these to test whether the electrodecremental response (increased high-frequency components concurrently with decreased low-frequency components of the spectra), in combination with any overt change in global synchrony (a measure of the degree of communication of activity in any given channel with the rest of the cortex under the electrode grid), could be a useful measure for seizure onset. Fig. 3B shows that, in this example, this was indeed the case. The FI, the ratio

of high spectral power to low spectral power multiplied by the synchrony, showed a clear local maximum corresponding to the beginning of the electrodecremental response. Preictal baseline scores were very low (mean 0.002 ± 0.002), and the peak score for the example shown was 2.453, a 1000-fold increase peaking at 17.0 seconds. Smaller increases were seen, decreasing in magnitude as the seizure progressed, but interestingly only the very late afterdischarges were associated with positive FI scores. With a nominal temporal resolution of 50 ms (the sliding window increment), we compared FI scores on all 32 channels, with an arbitrary lower threshold value of 1.0 (Fig. 3C). In this example the peak FI score was achieved only by a single electrode (No. 21) at a single time (17.0 seconds). From this time point, lower-value FI scores were seen radiating in an approximately spiral manner from electrode 21, a pattern typical of activity spread in uniform excitable media [33]. The key observation here, however, was that a single spatiotemporal origin from the electrographic seizure appeared to be detected using the dynamic signatures described above. This locus was part of the tissue resected from this patient, and the patient was seizure free 3 months following surgery.

To perform further preliminary tests as to the usefulness of such a simple analysis method, we examined, post hoc, electrocorticographic data from a second patient whose initial surgical resection was not fully successful. Fig. 4A shows an 80-second example of an electrographic seizure taken from channel 37 of the 48-channel array used with this patient. The subjective estimate of seizure onset again showed an electrodecremental signature, followed by slower repetitive burst discharges and absence of late afterdischarges in this case. The FI score changed over time in a manner similar to the example from patient A. Fifteen seconds into the example shown there was an abrupt, brief increase in FI score on this electrode (Fig. 4B). The average baseline FI score was 0.004 ± 0.003, and this increased to a local maximum of 4.982 on this channel, again a change of more than 1000-fold. As the seizure progressed a long-lasting increase in index was seen, but this rarely exceeded the arbitrary lower threshold of 1.0 for the duration of the event. When the FI score for all 48 channels was plotted, a spatiotemporal pattern different from that for patient A was seen. In this case two spatially separate main areas of highest FI score were seen. The largest was in a band from electrodes 29 through 37 to 46, but a more diffuse, concurrent increase was seen around electrode 42 at the very edge of the grid. In addition, smaller FI scores were obtained on a number of electrodes distributed across the entire grid, which returned to baseline for several seconds before reappearing, seemingly randomly throughout the area of cortex analyzed (Fig. 4C). Thus, in this case the focus index revealed multiple concurrent loci active at onset of seizure, suggesting a more diffuse extent to the underlying epileptogenic pathology.

4. Discussion

The present brief examples demonstrate that basic dynamic changes in focal epilepsies of neocortical origin may be useful in localizing the origin of observed electrographic seizures. Quantification of the electrodecremental response, coupled with a measure of how cortical areas communicate with each other through synchrony [34], allows transient changes in dynamics to be seen that correspond to a seizure focus or foci. The changes seen were of sufficient brevity and magnitude to allow spatial localization with an accuracy of at least the grid electrode separation (minimally 1 cm). With such accuracy it is possible to detect the presence of multiple foci under a single grid, which may be of use in improving outcomes of surgery for epilepsy. For example, detection of the absence of a focus in an area presumed to be responsible for the behavioral signature of a particular epilepsy [35], detection of dominant foci by analysis of multiple seizures from one patient in whom there are multiple foci [36], and detection of migratory foci [37] may all be possible.

The precision of focus detection using the present method may be explained by the dynamics of the main components used to construct the focus index score. Very fast oscillations have

been shown to be highly focal in origin [29], with multiple, spatially separate locations sometimes coexistent in the same lobe [26]. These VFOs are readily generated in very small areas of brain tissue maintained in vitro and can be reproduced with high fidelity in computational models consisting of only a few hundred neurons [38]. Gamma rhythms also have highly local neuronal network generators in neocortex [39], and increases in gamma power and synchrony occur locally in epilepsy [22,23]. Clues to why the occurrence of these rhythms at high powers is associated with the electrodecremental response come from multiple sources: In humans, DC EEG recording reveals DC shifts localized to a few electrodes associated with the electrodecremental response (i.e., occurring earlier than the "conventional" ictal EEG changes) [40]. Such DC shifts have been suggested to represent long-lasting (several seconds) depolarization of cortical neurons [41]. Experimental models of VFO and gamma rhythms also reveal association with long-lasting neuronal depolarization. VFOs are seen prominently at the beginning of up-states, a rhythmically occurring plateau depolarization associated with sleep in cat neocortex [42]. Gamma rhythms can occur persistently at low amplitude with no accompanying depolarization of cortical neurons [43]. However, much larger, transient field potential gamma rhythms are seen following stimulation that generates several seconds of depolarization in principal cells and interneurons [44]. Fig. 5 is a cartoon of composite electrophysiological recordings suggesting that the pattern of occurrence of the electrodecremental response fits with the initial “tonic” phase (i.e., plateau depolarization) of ictaform events recorded in individual cortical pyramidal cells. It is tempting therefore to speculate that the loss of low-frequency activity may be a consequence of such tonic depolarizations, with many of the cellular mechanisms underlying slow cortical rhythms being dependent on intrinsic conductances with strong membrane potential dependence. Given that DC shifts tend to be more spatially localized than the conventional ictal EEG pattern, this may further underlie the apparently good spatial resolution of the present focus index score.

By deliberately concentrating on a few features recognized as accompanying certain types of seizures, the method is clearly unlikely to be of use as a general screening tool for epileptiform activity. The above preliminary findings suggest a high degree of spatial resolution when used for seizures with initial electrodecremental response. This resolution was sufficient to distinguish an apparent unifocal epilepsy (patient A) from one of more diffuse, multifocal origin (patient B). It is interesting to note that patient A was seizure free following surgical resection, whereas patient B needed a second round of surgery to remove more cortical tissue. This suggested that the focus index may be useful in guiding surgery, or even indicating whether surgery is appropriate at all. However, the method also needs to be used on many further examples of different seizure types, multiple seizures from single patients, and needs to be compared with other seizure localization algorithms for validation. This work is ongoing and it is hoped that subsequent refinements on this theme may be of general use in localizing neocortical foci in epilepsies associated with many primary pathologies.

Acknowledgments

We thank the Wolfson Foundation and the MRC (Milstein award) for financial assistance.

References

1. Wiener, N. Cybernetics or control and communication in the animal and the machine. MIT Press; Cambridge: 1968.
2. Mars NJ, Lopes da Silva FH. Propagation of seizure activity in kindled dogs. Electroencephalogr Clin Neurophysiol 1983;56:194–209. [PubMed: 6191951]
3. Mukovski M, Chauvette S, Timofeev I, Volgushev M. Detection of active and silent states in neocortical neurons from the field potential signal during slow wave sleep. Cereb Cortex 2007;17:400–14. [PubMed: 16547348]

4. Fisher RS, Webber WR, Lesser RP, Arroyo S, Uematsu S. High-frequency EEG activity at the start of seizures. J Clin Neurophysiol 1992;9:441–8. [PubMed: 1517412]
5. Gotman J, Wang LY. State-dependent spike detection: concepts and preliminary results. Electroencephalogr Clin Neurophysiol 1991;79:11–9. [PubMed: 1713547]
6. Khan YU, Gotman J. Wavelet based automatic seizure detection in intracerebral electroencephalogram. Clin Neurophysiol 2003;114:898–908. [PubMed: 12738437]
7. Baier G, Muller M, Stephani U, Muhle H. Characterising correlation changes of complex pattern transitions: the case of epileptic activity. Phys Lett A 2007;363:290–6.
8. Ghosh-Dastidar S, Adeli H, Dadmehr N. Principal component analysis-enhanced cosine radial basis function neural network for robust epilepsy and seizure detection. IEEE Trans Biomed Eng 2008;55:512–8. [PubMed: 18269986]
9. Le van Quyen M, Adam C, Baulac M, Martinerie J, Varela FJ. Nonlinear interdependencies of EEG signals in human intracranially recorded temporal lobe seizures. Brain Res 1998;792:24–40. [PubMed: 9593809]
10. Le van Quyen M, Soss J, Navarro V, et al. Preictal state identification by synchronisation changes in long-term intracranial EEG recordings. Clin Neurophysiol 2005;116:559–68. [PubMed: 15721070]
11. Ochi A, Otsubo H, Donner EJ, et al. Dynamic changes of ictal high-frequency oscillations in neocortical epilepsy: using multiple band frequency analysis. Epilepsia 2007;48:286–96. [PubMed: 17295622]
12. Jerger, KK.; Netoff, TI.; Francis, JT., et al. Comparison of methods for seizure detection. In: Milton, J.; Jung, P., editors. Epilepsy as a dynamic disease. Springer; Berlin: 2003. p. 237-46.
13. Elger CE, Lehnertz K. Seizure prediction by non-linear times series analysis of brain electrical activity. Eur J Neurosci 1998;10:786–9. [PubMed: 9749744]
14. Martinerie J, Adam C, Le van Quyen M, et al. Epileptic seizures can be anticipated by non-linear analysis. Nat Med 1998;4:1173–6. [PubMed: 9771751]
15. Manuca R, Casdagli MC, Savit RS. Nonstationarity in epileptic EEG and implications from neural dynamics. Math Biosci 1998;147:1–22. [PubMed: 9401349]
16. Worrell GA, Parish L, Cranstoun SD, Jonas R, Baltuch G, Litt B. High-frequency oscillations and seizure generation in neocortical epilepsy. Brain 2004;127:1496–506. [PubMed: 15155522]
17. Allen PJ, Fish DR, Smith SJ. Very high-frequency rhythmic activity during SEEG suppression in frontal lobe epilepsy. Electroencephalogr Clin Neurophysiol 1992;82:155–9. [PubMed: 1370786]
18. Alarcon G, Binnie CD, Elwes RD, Polkey CE. Power spectrum and intracranial EEG patterns at seizure onset in partial epilepsy. Electroencephalogr Clin Neurophysiol 1995;94:326–37. [PubMed: 7774519]
19. Bragin A, Engel J Jr, Wilson CL, Fried I, Buzsaki G. High-frequency oscillations in human brain. Hippocampus 1999;9:137–42. [PubMed: 10226774]
20. Bragin A, Wilson CL, Staba RJ, Reddick M, Fried I, Engel J Jr. Interictal high-frequency oscillations (80–500 Hz) in the human epileptic brain: entorhinal cortex. Ann Neurol 2002;52:407–15. [PubMed: 12325068]
21. Draguhn A, Traub RD, Bibbig A, Schmitz D. Ripple (approximately 200-Hz) oscillations in temporal structures. J Clin Neurophysiol 2000;17:361–76. [PubMed: 11012040]
22. Ebersole JS, Pacia SV. Localisation of temporal lobe foci by ictal EEG patterns. Epilepsia 1996;37:386–99. [PubMed: 8603646]
23. Lee SA, Spencer DD, Spencer SS. Intracranial EEG seizure onset patterns in neocortical epilepsy. Epilepsia 2000;41:297–307. [PubMed: 10714401]
24. Avoli M, Biagini G, de Curtis M. Do interictal spikes sustain seizures and epileptogenesis? Epilepsy Curr 2006;6:203–7. [PubMed: 17260060]
25. Gupta D, James CJ. Narrowband vs broadband phase synchronisation analysis applied to independent components of ictal and interictal EEG. Conf Proc IEEE Eng Med Biol Sci 2007:3864–7.
26. Canolty RT, Edwards E, Dalal SS, et al. High gamma power is phase locked to theta oscillations in human neocortex. Science 2006;313:1626–8. [PubMed: 16973878]

27. Traub RD, Cunningham MO, Gloveli T, et al. GABA-enhanced collective behaviour in neuronal axons underlies persistent gamma-frequency oscillations. Proc Natl Acad Sci USA 2003;100:11047–52. [PubMed: 12960382]
28. Whittington MA, Traub RD. Inhibitory interneurons and network oscillations in vitro. Trends Neurosci 2004;26:676–82. [PubMed: 14624852]
29. Bragin A, Wilson CL, Staba RJ, Reddick M, Fried I, Engel J Jr. Interictal high-frequency oscillations (80–500 Hz) in the human epileptic brain: entorhinal cortex. Ann Neurol 2005;52:407–15. [PubMed: 12325068]
30. Bragin A, Wilson CL, Fields T, Fried I, Engel J Jr. Analysis of seizure onset on the basis of wideband EEG recordings. Epilepsia 2005;46:59–63. [PubMed: 15987255]
31. Traub RD, Whittington MA, Buhl EH, et al. A possible role for gap junctions in generation of very fast EEG oscillations preceding the onset of, and perhaps initiating, seizures. Epilepsia 2001;42:153–70. [PubMed: 11240585]
32. Mormann F, Kreutz T, Andrzejak RG, David P, Lehnertz K, Elger CE. Epileptic seizures are predicted by a decrease in synchronisation. Epilepsy Res 2003;53:173–85. [PubMed: 12694925]
33. Winfree AT. Spiral waves of chemical activity. Science 1972;175:634–6. [PubMed: 17808803]
34. Womelsdorf T, Schoffelen JM, Oostenveld R, et al. Modulation of neuronal interactions through synchronisation. Science 2007;316:1609–12. [PubMed: 17569862]
35. Babb TL, Halgren E, Wilson C, Engel J, Crandall P. Neuronal firing patterns during the spread of an occipital lobe seizure to the temporal lobes in man. Electroencephalogr Clin Neurophysiol 1981;51:104–7. [PubMed: 6161774]
36. Bailey P, Gibbs FA. The surgical treatment of psychomotor epilepsy. JAMA 1951;145:365–70.
37. Takashi I, Miura K, Nomura K, et al. Seizure prognosis and EEG evolution in complex partial seizures of childhood onset. Brain Dev 1990;12:498–502. [PubMed: 2288381]
38. Traub RD, Contreras D, Whittington MA. Combined experimental/simulation studies of cellular and network mechanisms of epileptogenesis. J Clin Neurophysiol 2005;22:330–42. [PubMed: 16357637]
39. Roopun AK, Middleton SJ, Cunningham MO, et al. A beta-2 frequency (20–30 Hz) oscillation in nonsynaptic networks of somatosensory cortex. Proc Natl Acad Sci USA 2006;103:15646–50. [PubMed: 17030821]
40. Ikeda A, Terada K, Mikuni N, et al. Subdural recording of ictal DC shifts in neocortical seizures in humans. Epilepsia 1996;37:662–74. [PubMed: 8681899]
41. Ayala GF, Dichter M, Gumnit RJ, Matsumoto H, Spencer WA. The genesis of epileptic interictal spikes. Brain Res 1973;52:1–17. [PubMed: 4573428]
42. Grenier F, Timofeev I, Steriade M. Neocortical very fast oscillations (ripples, 80-200 Hz) during seizures: intracellular correlates. J Neurophysiol 2003;89:841–52. [PubMed: 12574462]
43. Traub RD, Bibbig A, Fisahn A, LeBeau FEN, Whittington MA, Buhl EH. A model of gamma frequency network oscillations induced in the rat CA3 region by carbachol in vitro. Eur J Neurosci 2000;12:4093–106. [PubMed: 11069606]
44. Whittington MA, Doheny HC, Traub RD, Buhl EH. Differential expression of synaptic and non-synaptic mechanisms underlying stimulus-induced gamma oscillations in vitro. J Neurosci 2001;21:1727–38. [PubMed: 11222662]
45. Trevelyan AJ, Sussillo D, Watson BO, Yuste R. Modular propagation of epileptiform activity: evidence for an inhibitory veto in neocortex. J Neurosci 2006;26:12447–55. [PubMed: 17135406]

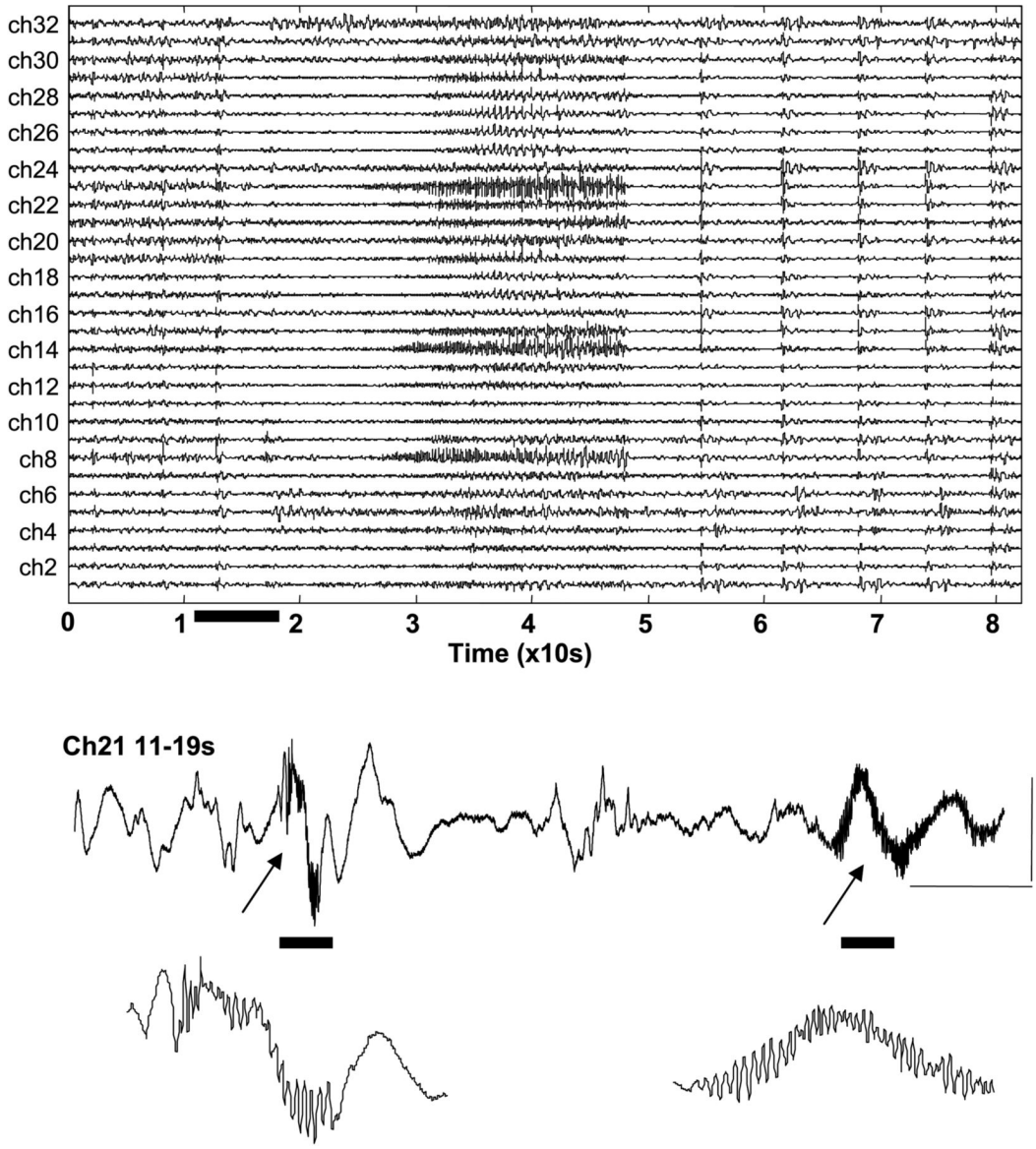

Fig. 1.

Basic features of electrocorticographic waveforms around seizure onset in patient 1. Recordings from 32 channels showing a reduction in ongoing low-frequency activity abruptly on most channels around 13 seconds into the example shown. A single channel is shown here for the 8 seconds during which slow activity ceases. Note the initial burst accompanied by fast oscillations (>80 Hz) resembling interictal-like activity, followed by a lower-amplitude burst with more protracted, higher-power fast oscillations that continues for several seconds (arrows). Scale bars = 0.1 mV, 1 second. The bottom two traces represent further extension of the time base, revealing the high-frequency oscillations in more detail.

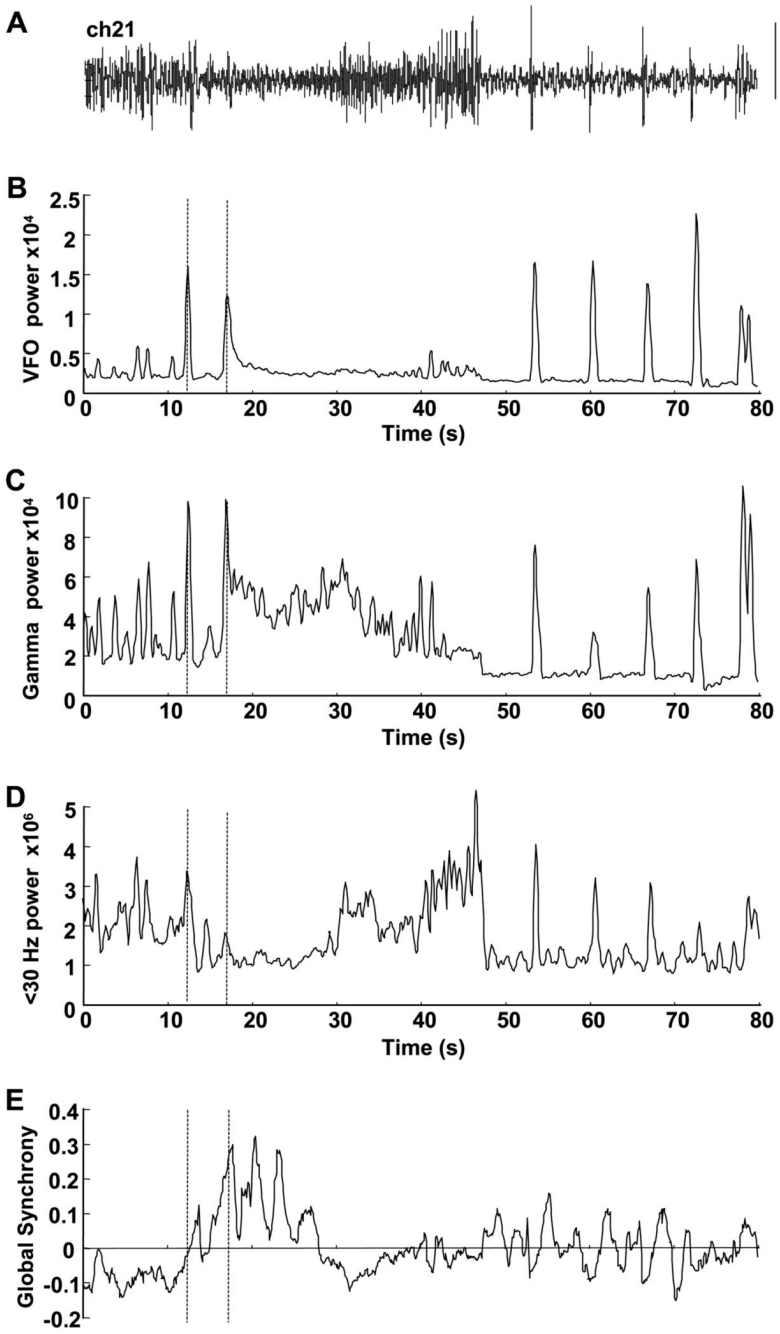

Fig. 2.

Dynamics of focus index components during seizure. (A) Electrocorticogram from channel 21 in patient A used to illustrate the patterns of change in frequency bands and global synchrony shown. An 80-second epoch is illustrated. Scale bar = 0.1 mV. (B) Peak VFO power from sliding window power spectral density estimate of bandpass-filtered data (80–500 Hz). (C) Gamma peak power from bandpass-filtered data (30–80 Hz). (D) Low-frequency peak power from windowed data bandpassed at 1–30 Hz. (E) Global synchrony measure for channel 21 during the 80-second epoch. Units for power are μV^2; synchrony units are arbitrary. Note none of these measures alone reveals changes unique at any single point during the transition from normal to ictal activity. Dashed lines show the time location of the two events highlighted in

the expanded trace in Fig. 1: the interictal-like event and the following onset of a long run of high-frequency rhythm.

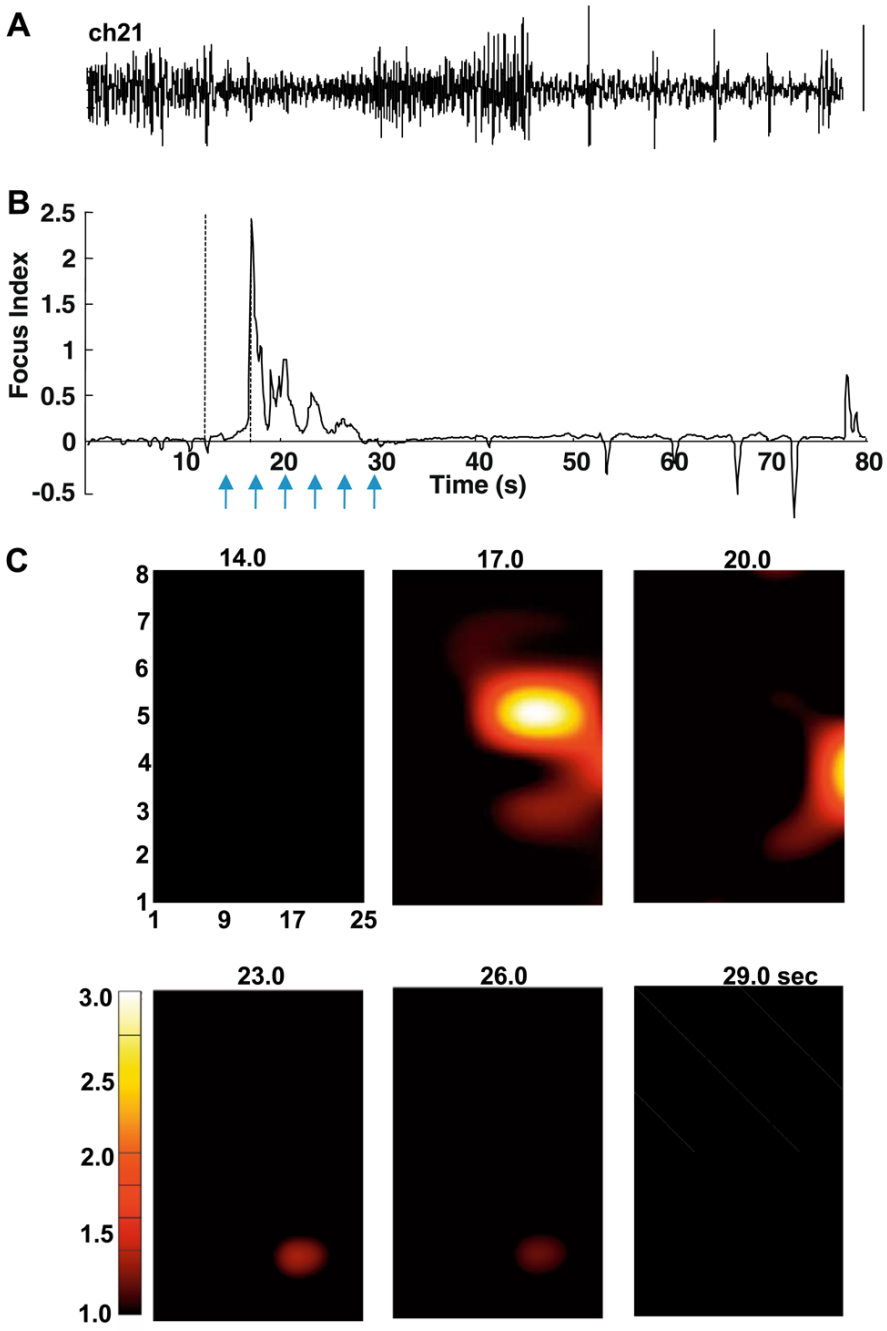

Fig. 3.

Focus index and focus localization for patient A. (A) Reproduction of raw electrocorticographic data from channel 21 for reference against the focus index. (B) The focus index changes over time for the channel in (A). Dashed lines indicate the time of the interictal-like response and onset of the electrodecremental response as in Fig 2. Note the large, transient positive score at 17.0 seconds corresponding to the onset of increased VFO and gamma power at that time, but no increase corresponding to the brief interictal-like event at 12.0 seconds (cf. Fig. 1, expanded trace). Arrows indicate the time points used for the grid examples below. (C) Time-specific maps of focus index score for all channels on the 32-channel grid used in this patient. Individual electrode scores were interpolated using cubic spline within the area of the

grid but not outside this area. Note that the high positive score “wanders” from the initial focus at electrode 21 to electrode 27 and electrode 18 in the first 9 seconds of the electrographic seizure event.

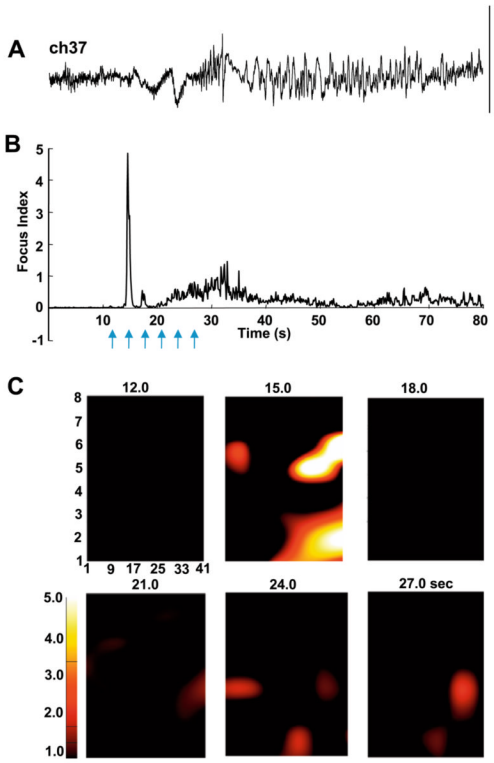

Fig. 4.

Focus index and focus localization for patient B. (A) Reproduction of raw electrocorticographic data from channel 37, 80-second epoch, for reference against the focus index. Scale bar = 0.2 mV. (B) The focus index changes over time for the channel in (A). Note the large, transient positive score at 15.0 seconds corresponding to the onset of increased VFO and gamma power at that time. The peak focus index score at this time contrasted sharply with values prior to the electrographic seizure, and was circa fivefold higher than at any other point during the seizure. Arrows indicate the time points used for the grid examples below. (C) Time-specific maps of focus index score for the 48-channel grid used in this patient. Individual electrode scores were interpolated within the area of the grid, but not outside this area. Note the high positive score is seen simultaneously in two main regions (electrodes 29/37/46 and around electrode 42 at the edge of the grid). Additional point sources for high focus index scores are also seen throughout the grid, both at the detected time point of initiation of the electrographic seizure and for several tens of seconds during the event.

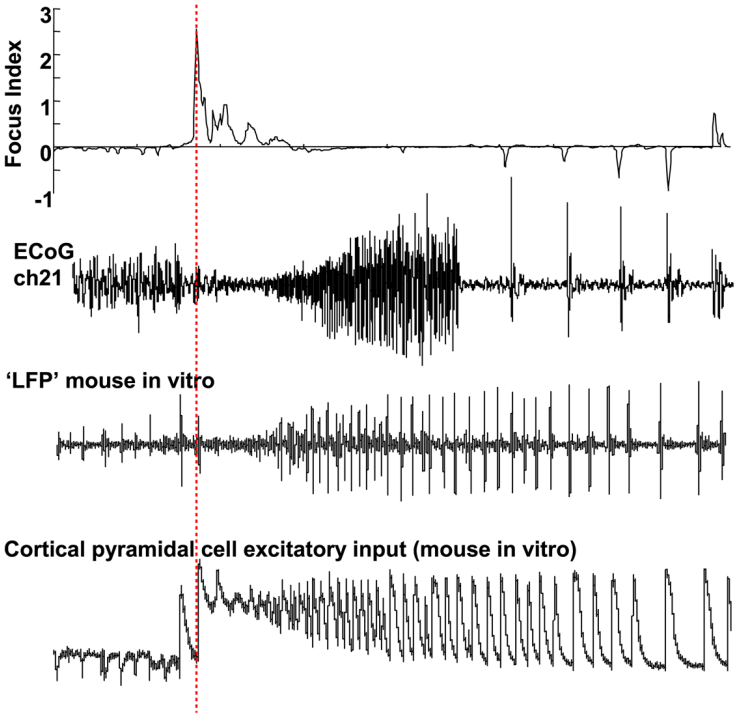

Fig. 5.

Cartoon comparing different types of seizure models with the detected focus in patient A. The focus index score and corresponding electrocorticogram for channel 21, patient A, are shown above with separately recorded examples of ictal-like events in animal models. The local field potential recording (LFP) illustrates an ictal-like event in mouse sensorimotor cortex activated with kainate 400 nM, under conditions of transient alkalinization of artificial cerebrospinal fluid (pH 7.4–8.4). The bottom trace is a recording of excitatory events in a cortical pyramidal neuron in the low extracellular magnesium model of cortical seizures [45]. Note in each "field recording" that an electrodecremental period precedes the generation of large-amplitude repetitive bursts at α–θ frequency. The pyramidal neuronal recording suggests that this population event may correspond to synchronous plateau depolarizations in cortical principal cells (see Section 4). Note the time scales of each example are not equal.